

MICROFABRICATED ELECTRODE ARRAYS SUITABLE FOR STIMULATION  
AND RECORDING IN CARDIAC ELECTROPHYSIOLOGICAL STUDIES

Except where reference is made to the work of others, the work described in this thesis is my own or was done in collaboration with my advisory committee. This thesis does not include proprietary or classified information.

---

Senthil Sivaswamy

Certificate of Approval:

---

Ramesh Ramadoss  
Assistant Professor  
Electrical and Computer Engineering

---

Thaddeus Roppel, Chair  
Associate Professor  
Electrical and Computer Engineering

---

Stuart Wentworth  
Associate Professor  
Electrical and Computer Engineering

---

Joe F. Pittman  
Interim Dean  
Graduate School

MICROFABRICATED ELECTRODE ARRAYS SUITABLE FOR STIMULATION  
AND RECORDING IN CARDIAC ELECTROPHYSIOLOGICAL STUDIES

Senthil Sivaswamy

A Thesis

Submitted to

the Graduate Faculty of

Auburn University

in Partial Fulfillment of the

Requirements for the

Degree of

Master of Science

Auburn, Alabama  
May 10, 2008

MICROFABRICATED ELECTRODE ARRAYS SUITABLE FOR STIMULATION  
AND RECORDING IN CARDIAC ELECTROPHYSIOLOGICAL STUDIES

Senthil Sivaswamy

Permission is granted to Auburn University to make copies of this thesis at its discretion, upon the request of individuals or institutions and at their expense. The author reserves all publication rights.

---

Signature of Author

---

Date of Graduation

## VITA

Senthil Sivaswamy, son of Sivaswamy Venkatachalam and Angathal Sivaswamy, was born on August 5, 1982, in Coimbatore, India. He entered Bharthiar University in 2000 and graduated from the Department of Electronic Engineering with the degree of Bachelor of Engineering in June, 2004. He entered the graduate program in the Department of Electrical and Computer Engineering in Auburn University in January, 2005.

## THESIS ABSTRACT

# MICROFABRICATED ELECTRODE ARRAYS SUITABLE FOR STIMULATION AND RECORDING IN CARDIAC ELECTROPHYSIOLOGICAL STUDIES

Senthil Sivaswamy

Master of Science, May 10, 2008  
(B.E Bharathiar University, Coimbatore, India, 2004)

51 Typed Pages

Directed by Thaddeus Roppel

Sudden cardiac arrest (SCA) caused by ventricular fibrillation is one of the most serious heart related problems in the United States today which is responsible for hundreds of thousands of deaths per year. The goal of this research project, a collaborative approach between Auburn University and the medical school in University of Alabama at Birmingham is to study the mechanisms responsible for the occurrence of sudden cardiac arrest. Due to the inherent electrical nature of the heart, a strong understanding of the electrical activity during the working of the heart is necessary to find the mechanisms that lead to SCA. The approach of this project is to design and fabricate microelectrode arrays for the measurement of surface potentials

in the heart tissue, which overcomes the limitations due to the spatial resolutions caused by the electrode arrays assembled manually using conductive wires. The microelectrode arrays are designed and fabricated in the electrical engineering department in Auburn University and the arrays are tested in the medical school at the University of Alabama at Birmingham. The approach used to design and fabricate the microelectrode arrays and the method of testing the arrays is included in the discussions. The results of the tests conducted on the microelectrode arrays support the use of this approach to be applied in the cardiac electrophysiological experiments.

## ACKNOWLEDGMENTS

I would like to thank Mr. Charles Ellis, Dr. Thaddeus Roppel and my advisory committee for supervising this thesis and supporting my graduate studies. I would like to thank my family for their continuing support towards my education.

Style manual or journal used: Graduate School Guide to Preparation of Thesis and  
Dissertations.

Computer software used: Microsoft Word 2003



## TABLE OF CONTENTS

|   |     |
|---|-----|
| LIST OF FIGURES .....                                       | x   |
| LIST OF TABLES .....  | xii |
| CHAPTER 1: INTRODUCTION .....                               | 1   |
| 1.1 Electro-physiology of heart.....                        | 1   |
| 1.2 Ventricular fibrillation .....                          | 3   |
| 1.3 Computing transmembrane current density .....           | 3   |
| 1.4 Microprobes for electrophysiological measurements ..... | 4   |
| 1.5 Microelectrodes for cardiac measurements .....          | 5   |
| 1.6 Impedance of the microelectrodes .....                  | 6   |
| 1.7 Buildings blocks of a microprobe .....                  | 8   |
| 1.8 Design of microprobes.....                              | 10  |
| CHAPTER 2: FABRICATION OF MICROELECTRODES.....              | 15  |
| 2.1 Fabrication Process .....                               | 15  |
| 2.2 Electrode Body Patterning .....                         | 15  |
| 2.3 Lift-off Process for Metal Deposition.....              | 17  |
| 2.4 Polyimide Application and Curing Process .....          | 18  |
| 2.5 Low Stress Curing of Polyimide Coating .....            | 19  |
| 2.6 Polyimide Layer Patterning .....                        | 20  |
| 2.7 Assembly of the Probes and Testing.....                 | 21  |
| CHAPTER 3: RESULTS AND DISCUSSIONS .....                    | 26  |
| 3.1 Fabrication Results.....                                | 26  |
| 3.2 Micro Impedance Measurements .....                      | 29  |
| 3.3 Potential Difference Measurements .....                 | 32  |
| 3.4 Signal Noise Measurements.....                          | 33  |
| 3.5 Noise Levels.....                                       | 34  |
| CHAPTER 4: CONCLUSIONS .....                                | 36  |
| REFERENCES .....  | 38  |

## LIST OF FIGURES

|  |    |
|--|----|
| 1.1 Electrical System of Heart .....   | 2  |
| 1.2 Equivalent Circuit for an Electrode Electrolyte Interface.....                   | 6  |
| 1.3 Equivalent Circuit for measuring electrode impedance.....                        | 7  |
| 1.4 Experimental set-up with microelectrode arrays and heart tissue .....            | 11 |
| 1.5 Schematic view of the electrode interface to heart tissue .....                  | 11 |
| 1.6 Layout of the electrode array .....  | 12 |
| 1.7 Linear array of electrodes .....   | 13 |
| 1.8 Electrode array designed with glass substrates.....                              | 14 |
| 2.1 Layout of the microelectrode array.....  | 16 |
| 2.2 Close-up view of the microelectrodes.....  | 17 |
| 2.3 Detailed cross section of the fabrication process.....                           | 25 |
| 3.1 Assembly of the electrode array .....  | 26 |
| 3.2 Close up view of platinum black electroplated arrays.....                        | 27 |
| 3.3 Electrode array in glass substrates with vacuum attachment.....                  | 28 |
| 3.4 Front side of the glass substrate showing four holes for vacuum attachment ..... | 28 |
| 3.5 Backside of the glass substrate with vacuum attachment hole in glass piece.....  | 29 |
| 3.6 Equivalent circuit for electrode impedance measurement.....                      | 30 |
| 3.7 Impedance versus frequency plot.....   | 31 |

|  |    |
|--|----|
| 3.8 Signal Noise Measurements for Surface Potentials.....          | 33 |
| 3.9 Signal Noise versus Frequency Plot for Surface Potentials..... | 35 |

## LIST OF TABLES

|   |    |
|---|----|
| 2.1 Polyimide application process ..... | 18 |
| 2.2 Polyimide curing process.....       | 19 |

# **CHAPTER 1**

## **INTRODUCTION**

Sudden cardiac arrest (SCA) is one of the most serious heart related problems in the United States today which is responsible for hundreds of thousands of deaths per year. The main reason for sudden cardiac arrest is ventricular fibrillation, which is a condition in the heart when the ventricles contract rapidly in an unsynchronized manner, which leads to a condition in which the heart is not able to pump blood into the body [1]. The aim of this research project, a collaborative effort between Auburn University and University of Alabama at Birmingham, is to design and fabricate microprobe arrays to be used in electrical recordings to investigate the mechanisms responsible for sudden cardiac arrest caused by ventricular fibrillation.

### **1.1 Electro-Physiology of the Heart**

The major components of the electrical structure of the heart are pacemaker cells found at the SA node, the specialized conduction tissue found at the AV junction and the cells of the atria and ventricles. The pacemaker cells found at the SA node are self excitatory which means following recovery, instead of maintaining a constant resting potential the trans-membrane potential increases until threshold is reached and an action potential takes place. As a result a regular succession of action potentials originates from

the SA node. These action potentials lead to a regular series of heart beats. The action potential initiated by the pacemaker cells excite neighboring cells, which leads to a cell to cell excitation in the atria. When the excitation reaches the AV node, specialized conduction cells carry the impulses into the ventricles. Since the ventricles and atria are separated by a specialized non conducting tissue, the excitation can reach ventricles from atria only through the AV node. These excitations cause the mechanical contractions of the heart muscles in an efficient and synchronized manner [2]. The schematic showing the specialized conduction system in the heart is shown in Figure 1.1

### Electrical System of the Heart

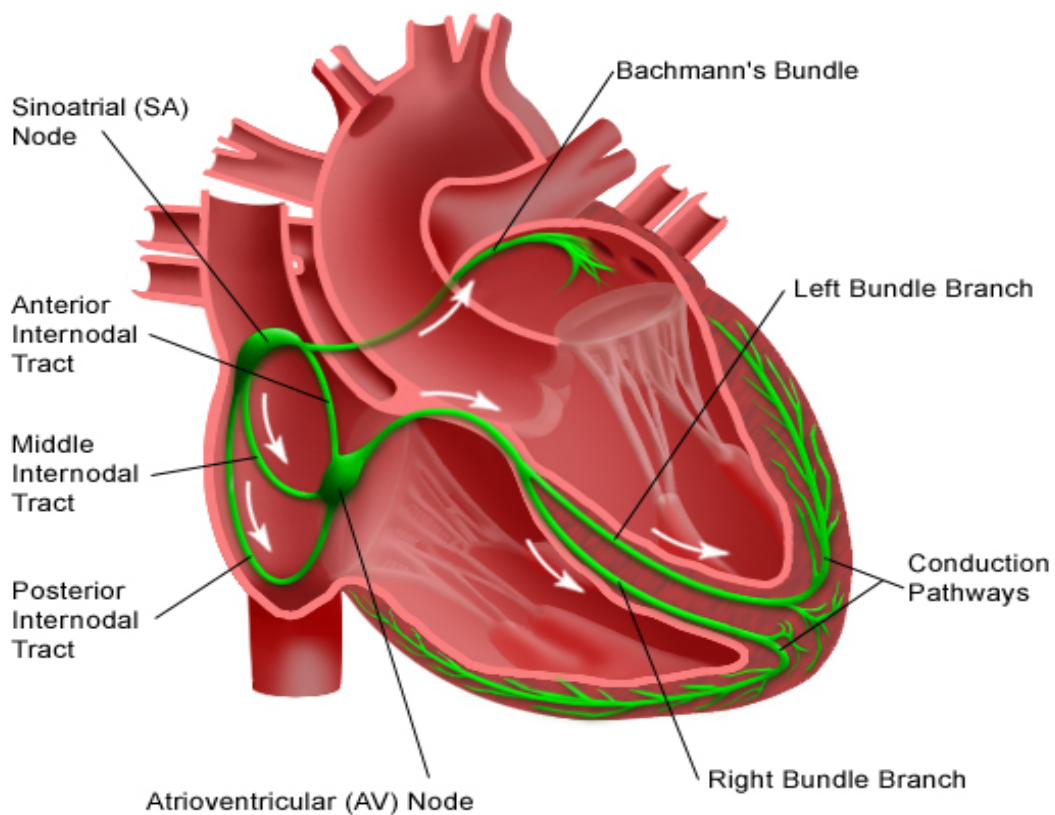


Figure 1.1 Electrical System of Heart

## **1.2 Ventricular Fibrillation**

Ventricular Fibrillation is a condition in the heart in which the heart beat becomes un-coordinated which results in ineffective pumping of the blood into the body, which leads to sudden cardiac death. The understanding of the mechanism that causes the ventricular fibrillation is very important to determine the causes and develop new therapies to cure the disease. Change in the balance of electrical source charge generation and the downstream load requirements is the reason for discontinuous conduction at the microscopic level, which leads to the onset of ventricular fibrillation[4].

## **1.3 Computing Trans-membrane current density**

Basic mechanisms that are responsible for the transition from uniform wave-front depolarization to highly discontinuous conduction at the microscopic level are not completely understood because of the lack of proper techniques for the computation of trans-membrane current density. Transmembrane current density depends on the sarcolemmal active currents and the passive current flowing in the interstitial, intracellular and extra cellular volume conductors. Transmembrane current density is a direct measure of electrical source and load influences on individual myocytes. Understanding the source-load relationships with the computation of the transmembrane current density would lead to a better understanding of the factors which causes change in the balance in the electrical source and load during the onset of ventricular fibrillation which then leads to sudden cardiac arrest [4].

Transmembrane current density  $I_m$  can be calculated from the following equation

$$I_m = -\frac{\partial}{\partial x}\left(g_{o,x} \frac{\partial \phi_o}{\partial x}\right) - \frac{\partial}{\partial y}\left(g_{o,y} \frac{\partial \phi_o}{\partial y}\right) - \frac{\partial}{\partial z}\left(g_{o,z} \frac{\partial \phi_o}{\partial z}\right) \quad (1)$$

Where  $g_o$  is the specific interstitial bio-domain conductivities in x, y and z directions.  $\phi_o$  is the interstitial potential.

Transmembrane current density computation has been simplified very much by the research studies showing that no intracellular access is required provided the surface potential gradients necessary can be measured in with sufficient spatial resolution as the size of individual myocytes. Microelectrode arrays are used to measure surface potentials. These can be built using well established microfabrication techniques. The required size of the electrodes and spacing between them as per the tissue architecture determine the required spatial resolution and accuracy of the position of the electrodes [4] [5].

#### 1.4 Microprobes for Electrophysiological Measurements

Microfabrication techniques have been used to fabricate microprobes which are used in many biomedical research applications such as electrophysiological studies in cardiac tissues, neurological stimulations and recording neural activity and in measuring intracellular ionic currents for drug discovery [4] [6] [7].

Prior to the use of microfabrication techniques, microelectrodes were built using conductive wires positioned into different geometric positions in the tissue during assembly. The disadvantage of this approach is when the electrode size is larger than



individual cardiac myocytes the resolution of the intrinsic electrical activity in the tissues becomes limited because the measurements reflect an averaging over multiple myocytes. Resolution is very important in these measurements because the electrical conduction in the tissues is influenced by changes in local electrical source-load relationship which depends on the cellular architecture [5]. With microfabrication techniques, electrode arrays can be built with precise size, shape and positions. Therefore measurements have very good spatial resolution and less tissue damage. The microprobes are easy to integrate with microelectronics circuitry when compared to traditional measurements made with wires.

### **1.5 Microprobes for Cardiac Measurements**

Electrophysiological studies directed towards understanding the mechanism of operation of the heart have the promise of identifying the potential causes of serious heart related diseases due to the inherent electrical nature of the heart. Internationally many research activities are under way to use electrodes built by micro fabrication techniques to investigate the electrical activity inside the heart. Cardiac recordings made with microelectrodes include measuring intramural potential differences during normal excitation and arrhythmias, to study discontinuous conduction at microscopic size scale, resolve microscopic electric fields and to compute trans-membrane current computation by measuring epicardial potential recordings. Chen et al have used ultrasonically activated silicon probes for recording cardiac activity inside the ventricular wall with 10 Mohm at 10 Hz with platinum sensors, Kim et al have used iridium probes on silicon substrates to record cardiac electrograms with 5 Mohm at 10 Hz with iridium sensors.

Pollard et al have used chloridized silver electrodes for measuring surface potentials with 1.2 Mohm at 10 Hz [4] [8] [9]. In this work, the primary goal is to decrease the effective impedance of the electrodes in order to improve the signal to noise ratio in the acquired data.

The electrodes required for cardiac measurements should have sufficient spatial resolution to resolve the microscopic propagation of the electrical activation and at the same time electrical impedance should be in the acceptable range without damaging the individual cells.

### **1.6 Impedance of the Microprobes**

Impedance of the microelectrodes is an important area of focus in design, material selection and fabrication of microelectrodes. The impedance of the microelectrodes depends on many factors such as the frequency of operation, resistivity of the electrode material and surface area of the electrode which is in contact with electrolyte [4] [7].

The impedance of the microelectrodes can be characterized by understanding the electrode- electrolyte interface. When the microelectrode is in contact with a conductive solution, the charge transfer from the electrode to the electrolyte occurs by faradic reactions and capacitive charging.

The equivalent circuit of an electrode electrolyte interface is shown in Figure 1.2

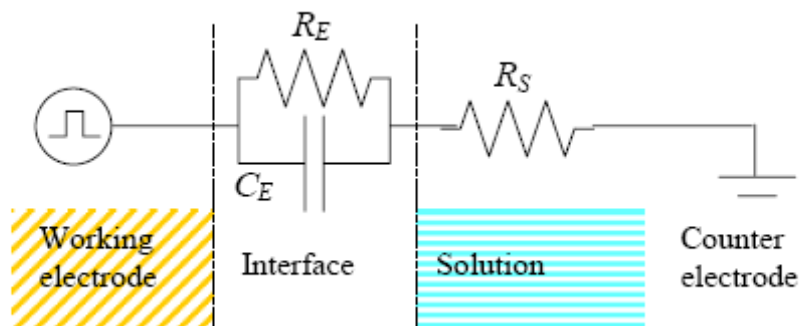


Figure 1.2 Equivalent circuit for an electrode electrolyte interface.

A faradic reaction is a heterogeneous charge-transfer reaction occurring at the surface of an electrode in electrode-electrolyte interface. It is the transfer of electrons from the ions in the solution by redox reactions of metal species. Capacitive charging occurs in the interface due to the accumulation of electrons in the electrodes surface and ions near the electrode in the solution. The resistance associated with faradic reaction is denoted by  $R_e$  and capacitance due to the capacitive charging is denoted by  $C_e$ . In Figure 1.2,  $R_s$  denotes the series resistance of the solution.

The effective impedance of the microelectrode can be determined by using the following circuit.

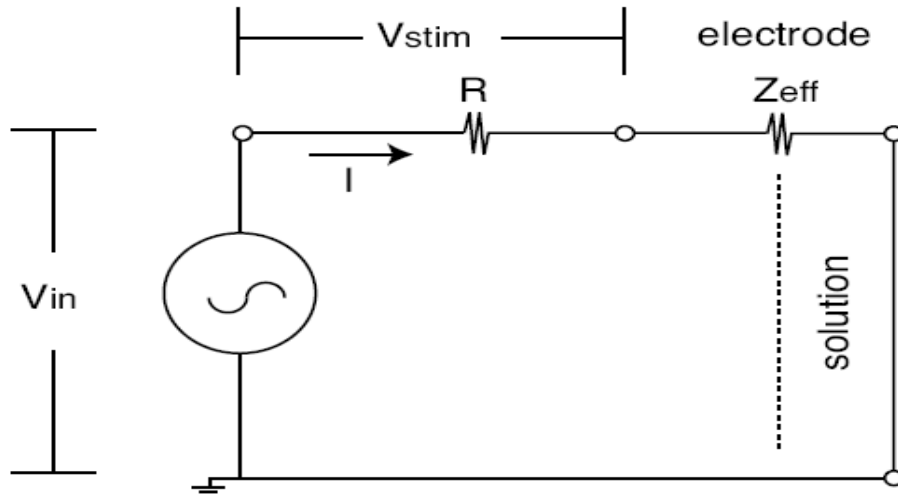


Figure 1.3 Equivalent circuit for measuring electrode impedance.

Where  $Z_{eff}$  includes the parallel resistive component due to faradic charging and capacitive component due to charging and the series resistance of the solution.  $R$  is the resistance of the electrode.

By solving the above circuit using Kirchhoff's voltage law the effective impedance of the microelectrode can be calculated by the following equation.

$$Z_{eff} = R \left( \frac{V_{in}}{V_{stim}} - 1 \right) \quad (2)$$

Where  $V_{in}$  is the input voltage and  $V_{stim}$  is the voltage drop across the known resistor  $R$ .

### 1.7 Building Blocks of Microprobes

The four essential parts of a microprobe are the supporting substrate, microelectrode array, the electrode interconnects and the insulating layer. Silicon is chosen as the substrate material for this work because it is widely used in micro fabrication techniques. Glass substrates were also used to fabricate these electrodes

because it is transparent and has the advantage of accurate positioning of the electrode during electrophysiological studies.

The microelectrode is the part of the probe that will be in direct contact with the tissue specimen and the conducting solution. The desired qualities of the material to be used in the electrode are biocompatibility, stability, low resistivity and durability. Platinum black, Iridium and Titanium nitride are the preferred choices for electrode materials used in electrophysiological studies.

Platinum black is deposited by electrodeposition using current crowding to a highly porous dendritic structure. The surface area of the electrode deposited by platinum black is very high when compared to the flat electrode area. The inherent advantage of using platinum black as electrode material over iridium and titanium nitride is that the increase in surface area is useful in fabricating low impedance electrodes due to its increased electrode surface area. The problems associated with choosing platinum black as the electrode material is that it has higher dissolution rates due to faradic reactions and the corresponding reduction in surface area which affects the electrode lifetime[10] [11]. Iridium is a very stable metal used in high temperature sensors. Its advantages are that it has many reversible oxidation states which deliver high faradic current and slow dissolution rates. The problems associated with iridium are it is slower when compared to platinum black in delivering current in stimulation applications and the deposition techniques to achieve robust electrode film are not available with electrodeposition. Titanium nitride is the other material choice for the electrode material. It is extremely durable and has high charge injection capacity. The use of titanium nitride as the

electrode material is very limited due to the lack of well documented deposition techniques [12].

Platinum black is chosen as the electrode material for this work because it can be easily electrodeposited and it meets the requirements such as stability, speed and impedance for the chosen application.

The electrode interconnects and the connecting pads are deposited using e-beam deposition of titanium, nickel, aluminum and gold. Gold is chosen as the conductor because it is easily solderable with the connecting wire. The insulating layer used in this work is polyimide. Polyimide is bio-compatible and it is easily deposited and patterned using existing micro fabrication techniques. The adhesion of polyimide to silicon and glass substrates can be increased by using adhesion promoter. Polyimide can absorb moisture and it affects the reliability of the insulating layer in long term usage. Proper curing of the polyimide film after deposition and careful handling of the film during measurements can minimize the problems associated with moisture absorption.

PDMS is the other alternative insulating layer because of its high chemical stability and has been used as an insulating layer in biomedical implants in heart valves. The mechanical strength and the adhesion of the PDMS films to silicon substrate is the limiting factor in using it as an insulating layer.

## **1.8 Design of Microprobes**

The experimental set up of the microelectrode array with heart tissue used for the measurement of surface potential is shown in figure 1.4. The close-up of the microelectrode array is placed on the surface of the heart tissue as shown in figure 1.5.

The electrode surface which is electroplated with platinum black comes into contact with the surface of the heart tissue which is immersed in a conductive solution.

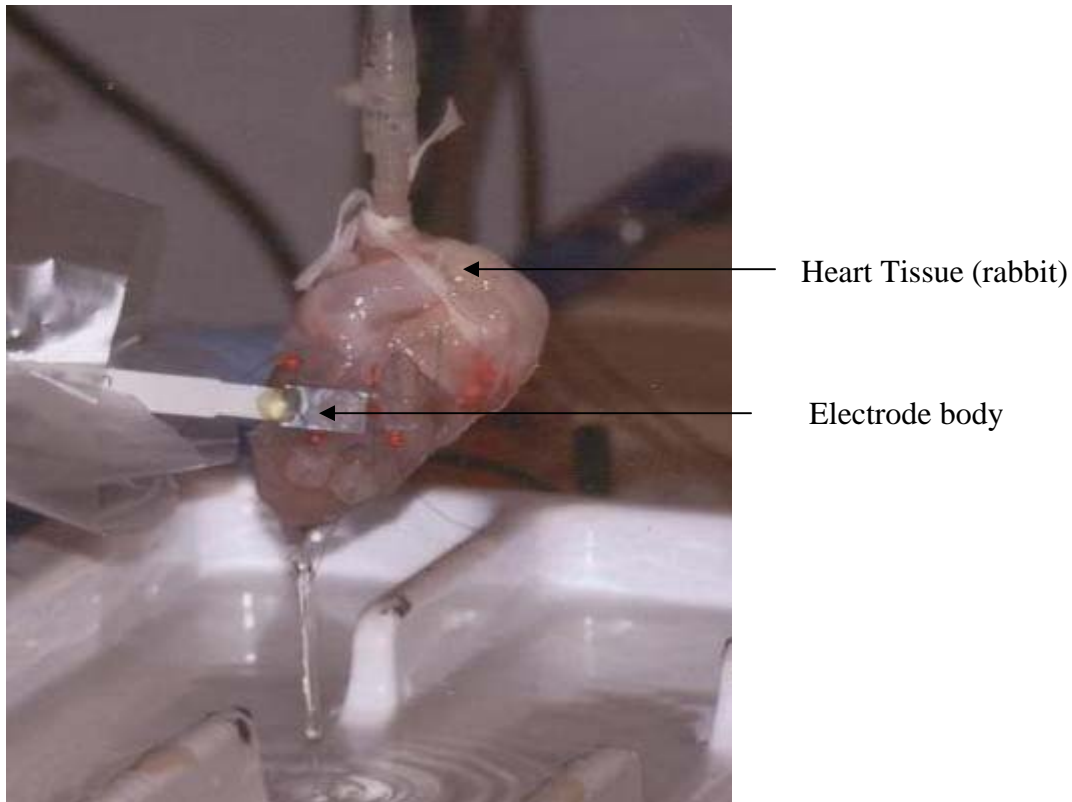


Figure 1.4 Experimental set-up with microelectrode arrays and heart tissue.

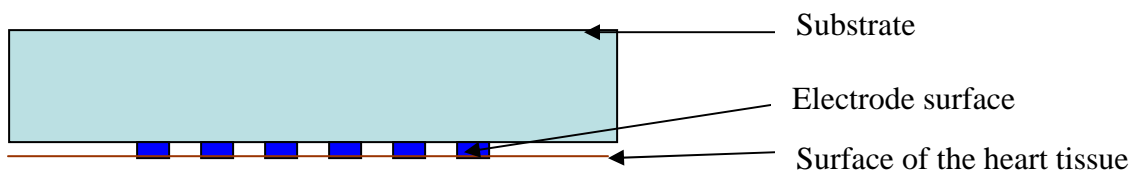


Figure 1.5 Schematic view of the electrode interface to heart tissue.

The placement of the microelectrodes is the key aspect in the design of the micro probe. Since the microelectrodes are the only part of the probe that is going to be in contact with the tissue under test, the placement, size and spacing of these electrodes decide the overall design. The other fixed part of the design is the connection pads which are used to solder the connection cables, which are commercially available. The

interconnecting metal traces connect the microelectrodes with the soldering pads. The size of the micro electrodes and the spacing between them is determined by the electrode impedance that is acceptable and by the required resolution for the measurement.

The design of the microprobe used for this work is shown in Figure 1.6. The electrode array is placed in one end of the substrate and the other end of the substrate contains the solder pads to the external connection cables. The size of the sensor substrate is determined by the number of electrodes in the array and the size of the solder pads.

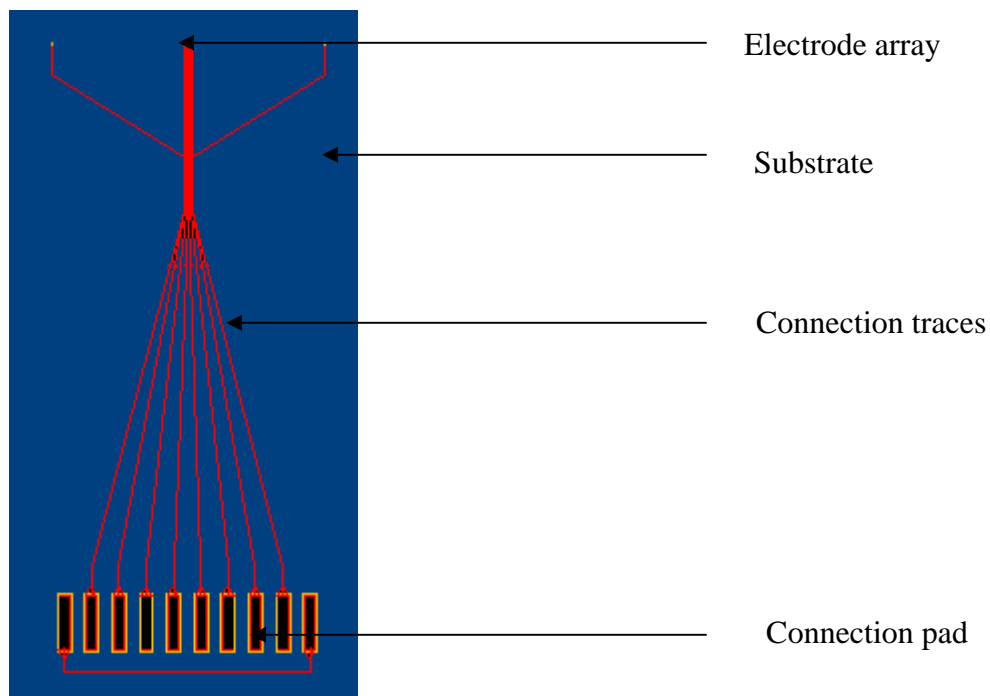


Figure 1.6 Layout of the electrode array.



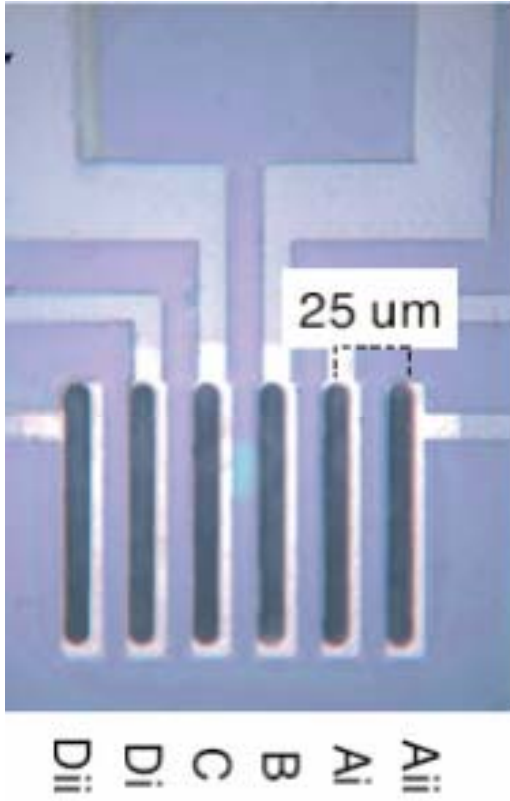


Figure 1.7 Linear array of electrodes.

There are eight electrodes of size  $5\ \mu\text{m}$  by  $150\ \mu\text{m}$  placed in this array. The six central electrodes are placed with  $25\ \mu\text{m}$  separation between each electrode. The electrodes are named Ai, Aii, B, C, Di, and Dii. The A and D electrodes are used for applying the stimulation and the other electrodes B, C are used to measure the potential differences caused by the stimulations.

The other design of the microprobes is with glass substrate shown in Figure 1.8.

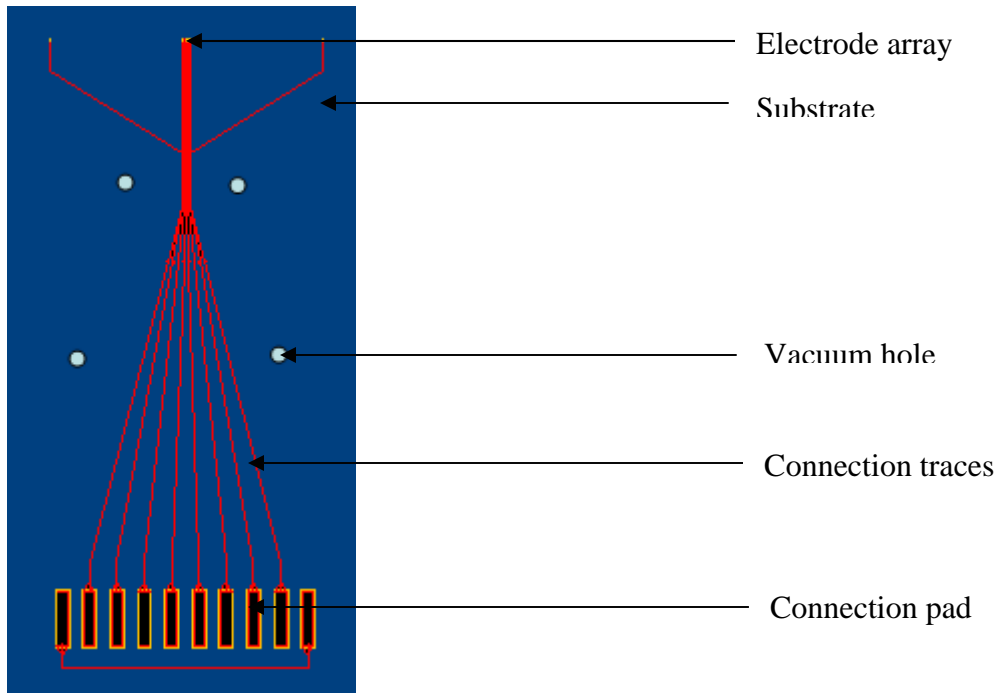


Figure 1.8 Electrode array designed with glass substrates.

The major difference in the probe designed with glass substrate is the probe is assembled with vacuum holes in the glass substrate. The vacuum holes are drilled in the glass substrate to attach the probe body to the heart tissue by pulling vacuum. The advantage of this design is that it eliminates the tissue damage caused by suturing the silicon probe body with the heart tissue and the glass substrate makes the placement of the electrodes easy because of its transparency.

## **CHAPTER 2**

### **FABRICATION OF MICROELECTRODES**

#### **2.1 Fabrication Process**

The fabrication of the microelectrodes involves two steps: fabricating the different designs of the microelectrodes on a silicon substrate, and assembling the probes with flexible connector and electroplating platinum black on the electrodes.

The microelectrodes are fabricated on 4-inch diameter silicon substrates. An insulating layer of oxide of thickness  $6000\text{\AA}$  is grown on the silicon substrate. The silicon wafers are oxidized in an oxidation furnace. The silicon wafers are loaded in the furnace and the oxidation performed in the presence of oxygen and hydrogen gases at  $1050\text{ }^{\circ}\text{C}$ .

#### **2.2 Electrode Body Patterning**

The oxidized silicon wafers are then patterned with a layer of positive photoresist to deposit the electrode array, connection traces and the connecting pads. Prior to the application of photoresist, the silicon wafers are placed in a dehydration oven at  $120\text{ }^{\circ}\text{C}$  for 20 minutes. Adhesion promoter solution HMDS is evaporated on the wafer surface

for 20 minutes to improve the adhesion between the oxide layer and the photoresist. A thin layer of positive photo resist AZ5214 is spun on the oxidized wafer at 3000 rpm for 30 seconds and it is soft baked at 110°C for 1 minute. Then the silicon wafer is patterned using the mask that is defined for the conducting lines and pads. The mask layout is shown in figure 2.1 and figure 2.2.

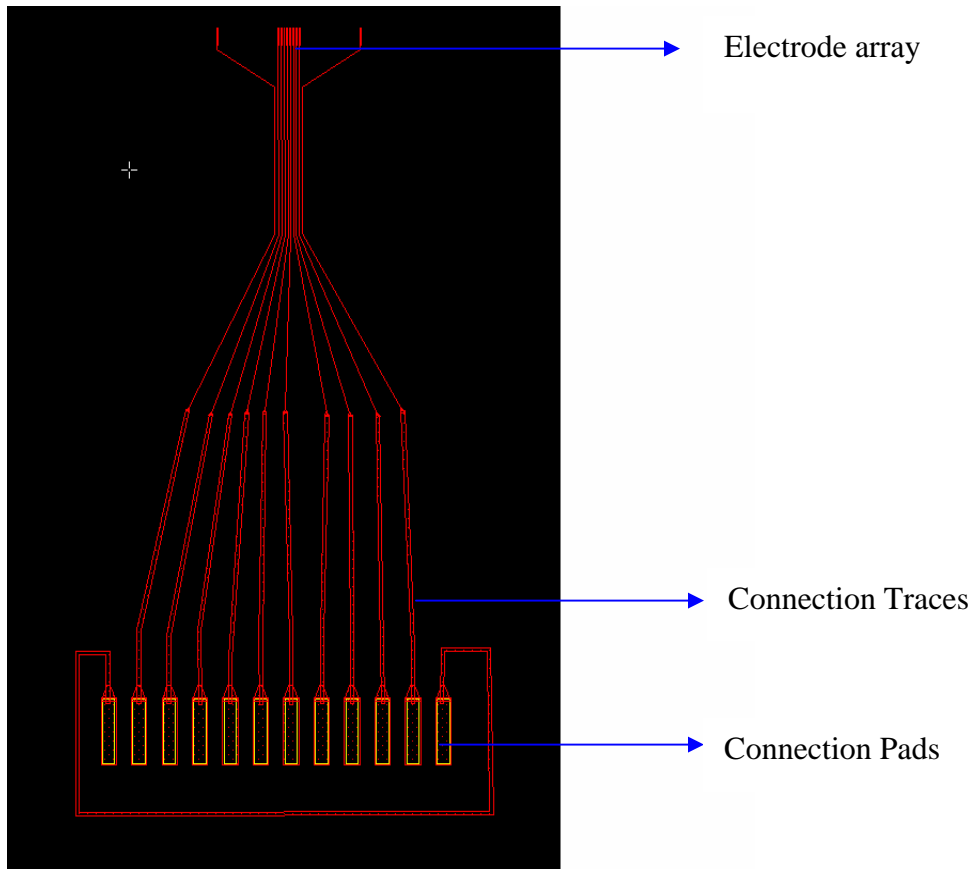


Figure 2.1 Layout of the microelectrode array.

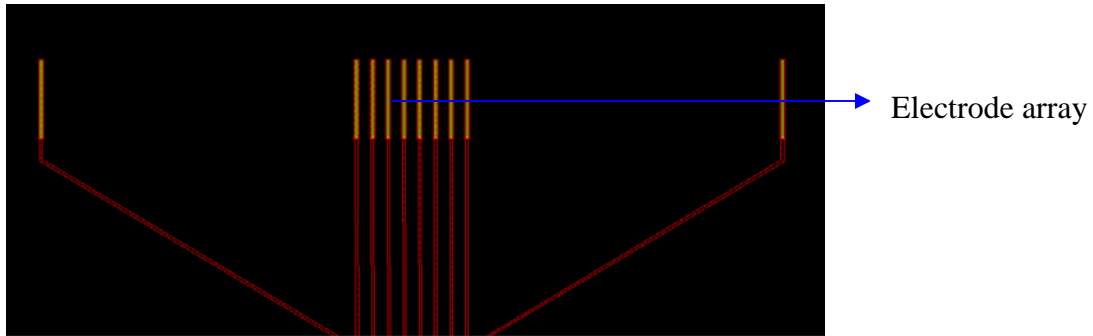


Figure 2.2 Close-up view of the microelectrodes

After exposing the substrate to ultraviolet light for 8 seconds, the photoresist layer is developed using AZ400 positive photoresist developer for 30 seconds in a solution containing 3 parts of deionized water to 1 part of AZ400 solution. After developing the photoresist, a plasma descum is performed to remove any residual photoresist. The patterned probes are shown in Figure 2.3b.

### 2.3 Lift-off Process for Metal Deposition

The next step is deposit thin layers of metals to form the electrodes, conducting traces and connection pads using e-beam deposition. Four layers of metal, aluminum, nickel, gold and chromium, are deposited. The aluminum layer ( $3000\text{\AA}$ ) is first deposited to improve the adhesion between the subsequent metal layers and to provide a stress release layer. Nickel ( $3000\text{\AA}$ ) is deposited to act as a solder base for the connecting pads. Gold ( $1000\text{\AA}$ ) is deposited as the main conductor metal for the electrodes and the connection pads and to act as an oxidation barrier for the nickel. Chrome ( $300\text{\AA}$ ) is deposited to protect the gold layer during processing.

After the e-beam deposition of metal layers a lift off process is performed by placing the silicon substrate in an ultrasonic bath containing acetone for 20 minutes. The cross section after the liftoff process is shown in Figure 2.3c.

## **2.4 Polyimide application and curing process**

### **Polyimide Application:**

The wafers are coated with Polyimide PI- 2611 from HD Microsystems to a thickness of 6  $\mu\text{m}$ . Adhesion promoter VM 651 from HD Microsystems is applied to the wafers to improve the adhesion of polyimide to the oxide layer. The following is the process used to spin coat polyimide for a thickness of 6  $\mu\text{m}$ . The resulting cross-section is shown in Figure 2.3d.

Table 2.1.Polyimide application process

### **Dehydration Bake**

Time: 30 minutes

Temperature: 120°C

### **Adhesion Promoter VM -651 Coating**

Step 1 Spin Speed: 500 rpm

Spin Time: 5 seconds

Step 2 Spin Speed: 3000 rpm

Spin Time: 30 seconds

### **Polyimide PI -2611 Application Coating**

Step 1 Spin Speed: 500 rpm

Spin Time: 5 seconds

Step 2 Spin Speed: 3000 rpm

Spin Time: 40 seconds

**Soft Bake**

Time: 5 minutes

Temperature: 120°C

**2.5 Low Stress Curing of Polyimide Coating:**

After coating the wafers with polyimide using the spin coating, they are loaded in a programmable nitrogen oven at ambient temperature. Table 2.2 is the process used to cure the polyimide layer under low stress.

Table 2.2.Polyimide application process

**Step 1**

Target Temperature: 90°C

Ramp rate: 1°C/min.

Curing Time: 30 minutes

**Step 2**

Target Temperature: 120°C

Ramp rate: 1°C/min.

Curing Time: 30 minutes

**Step3**

Target Temperature: 350°C

Ramp rate: 2°C/min.

Curing Time: 60 minutes

#### **Step 4**

The nitrogen oven is then cooled down to ambient temperature.

### **2.6 Polyimide Layer Patterning**

After the coating and curing of the polyimide layer, openings in the polyimide are etched in the electrodes and the connection pads. The polyimide etching is performed in STS Advanced Oxide Etching Systems by Deep Reactive Ion Etching. Prior to the application of photoresist the polyimide coated wafers are placed in dehydration oven in nitrogen for 20 minutes at 120°C, followed by 20 minutes in HMDS solution. A thin layer of aluminum masking layer (3000Å) is deposited by e- beam deposition. The next step is patterning probes using the photolithography. A thin layer of positive photo resist AZ5214 is spun on the oxidized wafer at 3000 rpm for 30 seconds and it is soft baked at 110°C for 1 minute. Prior to the application of photo resist the polyimide coated wafers are placed in dehydration oven in nitrogen for 20 minutes at 120°C, followed by 20 minutes in HMDS solution. The top view of the mask which shows the electrode openings is shown in Figure 2.2.

After exposing the substrate to ultraviolet light for 8 seconds, the photo resist layer is developed using AZ400 positive photo resist developer for 30 seconds in a solution containing 3 parts of DI water to 1 part of AZ400 solution. After developing the photo resist plasma, a de-scum is performed to remove any residual photo resist.

After patterning the probes, the aluminum mask is etched using by PAE solution for 5 minutes and 30 seconds. Polyimide is etched by reactive ion etching using the STS advanced oxide etcher.



After etching the polyimide layer the masking aluminum layer is removed by etching in PAE solution for 5 minutes and 30 seconds. The chrome layer is removed by using a chrome etchant CRE which exposes the gold layer for subsequent processes of soldering the connection pads and electroplating of platinum black. The resulting cross-section is shown in Figure 2.3f.

## **2.7 Assembly of the Probes and Testing**

After etching the chrome layer, the silicon wafer is diced to separate all the individual probe arrays. The next step is to assemble the probes with the flexible connector. Solder is applied to the contact pads and the connector is aligned with the contact pads precisely and it is soldered to the probe.

To prepare individual arrays for the experimental tests, flexible ribbon connection cables are soldered to each sensor body. For bonding, a small solder bump on each connection pad is aligned with the cable strands using a Plexiglass jig. The array, cable and jig are then placed into an oven to melt solder and form the bond. To further protect the bond, we covered the front and back side of the cable and sensor body is covered with epoxy. After the epoxy on the bond hardened, the full assembly is mounted into a connector on a breakout board. The electrode region of the sensor body is then immersed in a platinizing solution (YSI 3140, YSI, Yellow Springs, OH). Platinum black is electroplated using a 0.1 mA current for 10 seconds with 1.1 V potential difference between the anode and the cathode in platinizing solution. The resulting cross-section is shown in Figure 2.3g. Once plating was confirmed for all electrodes, the sensor body is again washed using methanol and dried using ethanol. The electroplating step also serves

as a test step since uniform electroplating in the electrodes confirm that the solder bond between the sensor connection pads and the connection cables is good and that the metal traces in the sensor body are continuous without any open metal traces. Assemblies are taped in plastic wafer containers and stored with the back of the sensor body in contact with the plastic surface to protect the electrodes in advance of experiments.

The detailed cross section photos of the fabrication process are shown in Figure 2.3.

Figure 2.3(a)

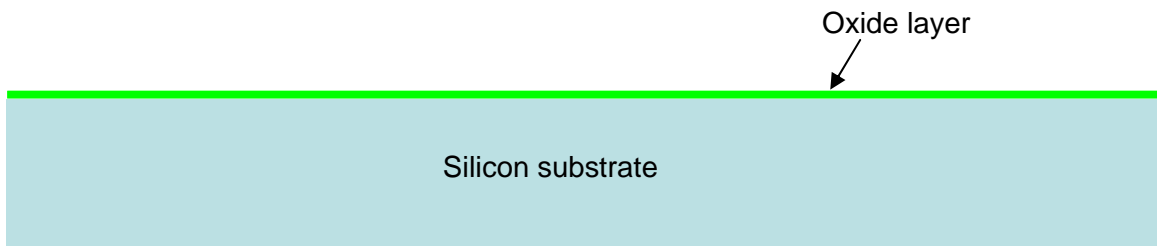


Figure 2.3(b)

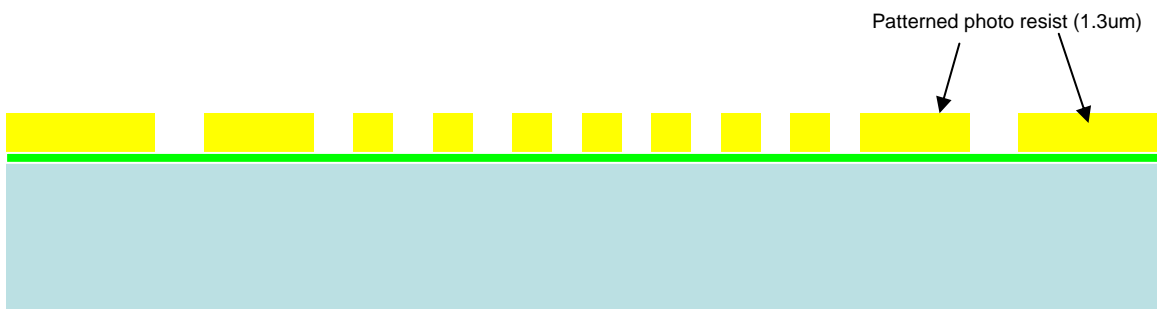


Figure 2.3(c)

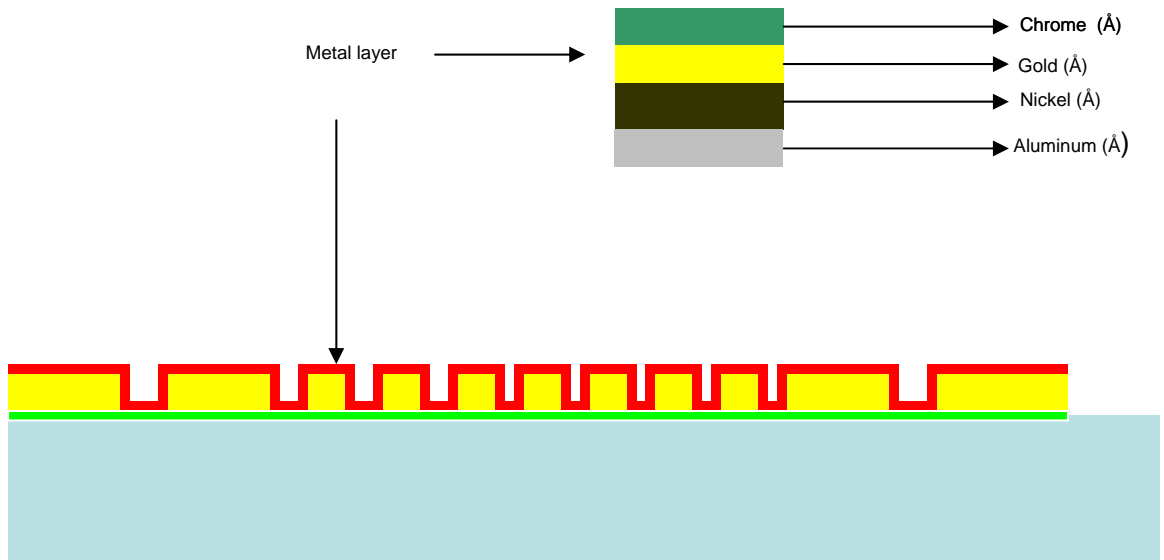


Figure 2.3(d)

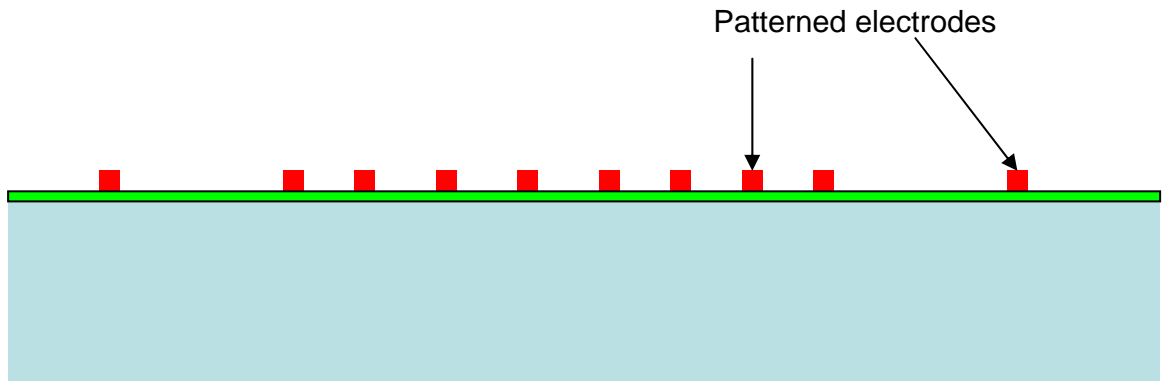


Figure 2.3(e)

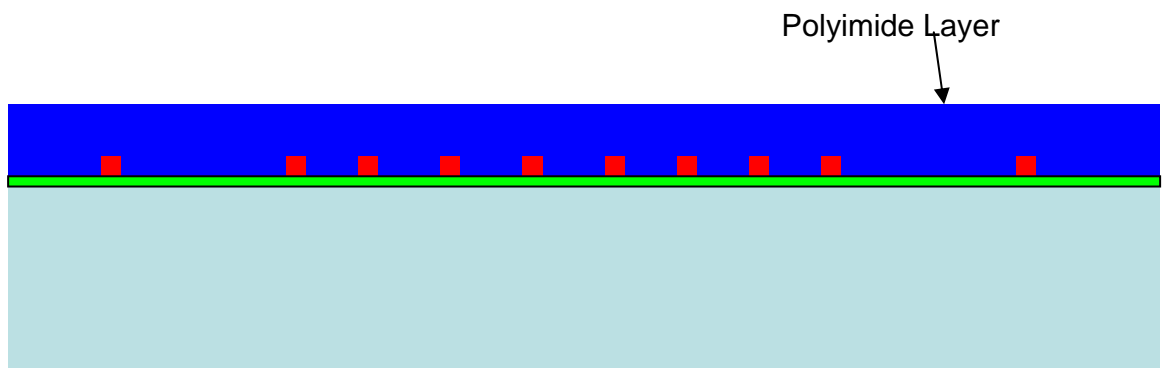


Figure 2.3(f)

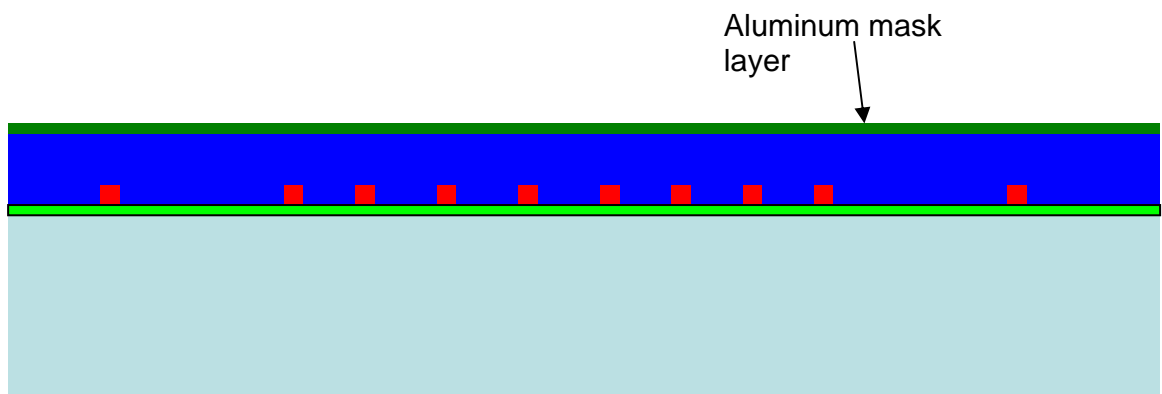


Figure 2.3(f)

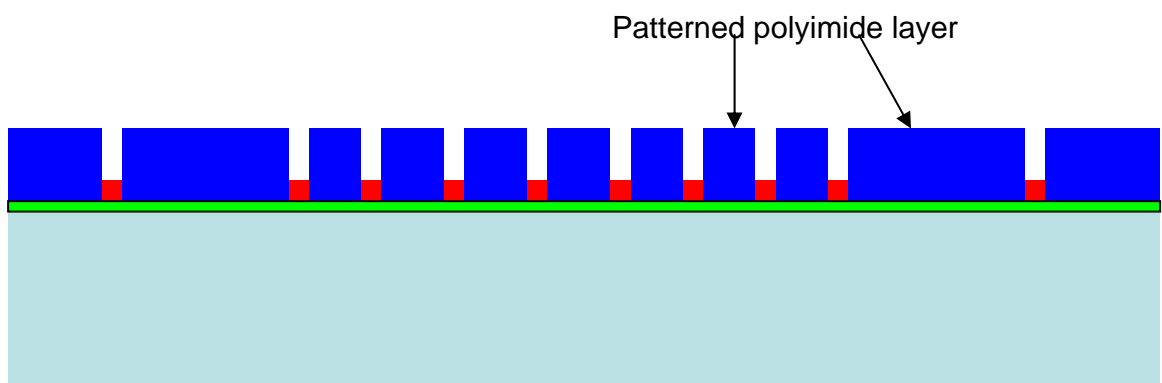


Figure 2.3(g)

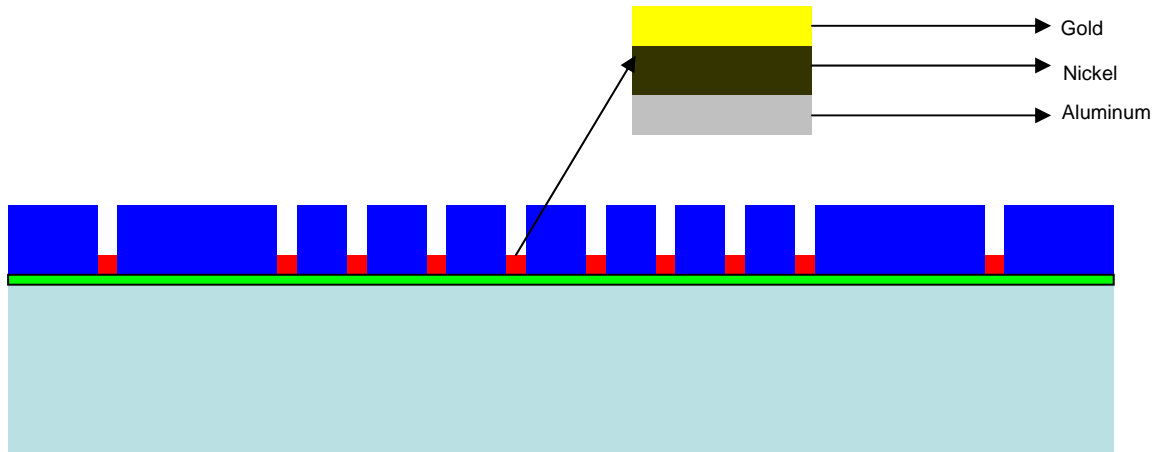


Figure 2.3(h)

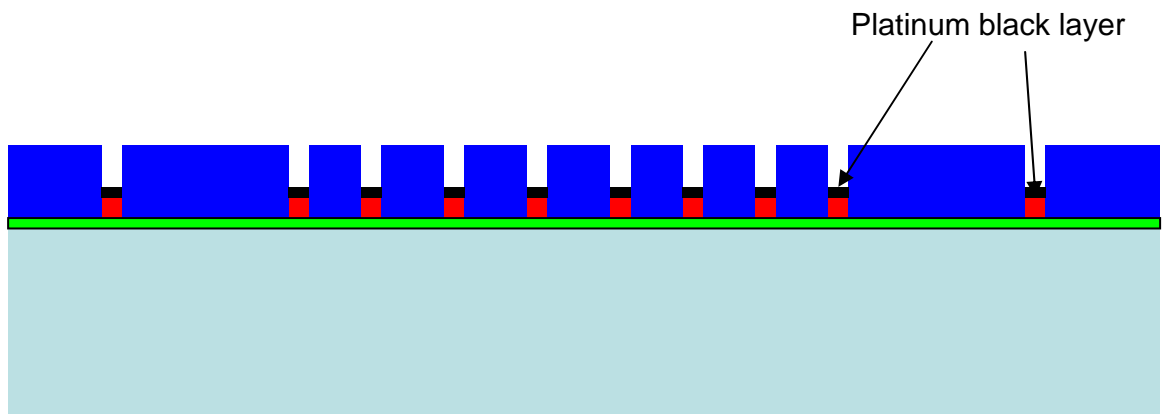


Figure 2.3 Detailed cross-section for the fabrication process, (a) Oxide layer deposition, (b) Electrode array patterning, (c) E-beam deposition of metals, (d) Lift-off Process, (e) Polyimide deposition and curing, (f) Aluminum mask layer deposition, (g) Patterned polyimide layer, (g) Chrome layer etching, (h) platinum black electroplating.

**CHAPTER 3**  
**RESULTS AND DISCUSSIONS**

**3.1 Fabrication results**

The electrical characteristics of the microelectrodes are tested in the cardiac rhythm management laboratory in the medical center of University of Alabama at Birmingham by Dr. Andy Pollard's research group.

The fabricated microelectrodes are assembled with the connecting wire using solder attachment. The final assembly is shown in Figure 3.1.

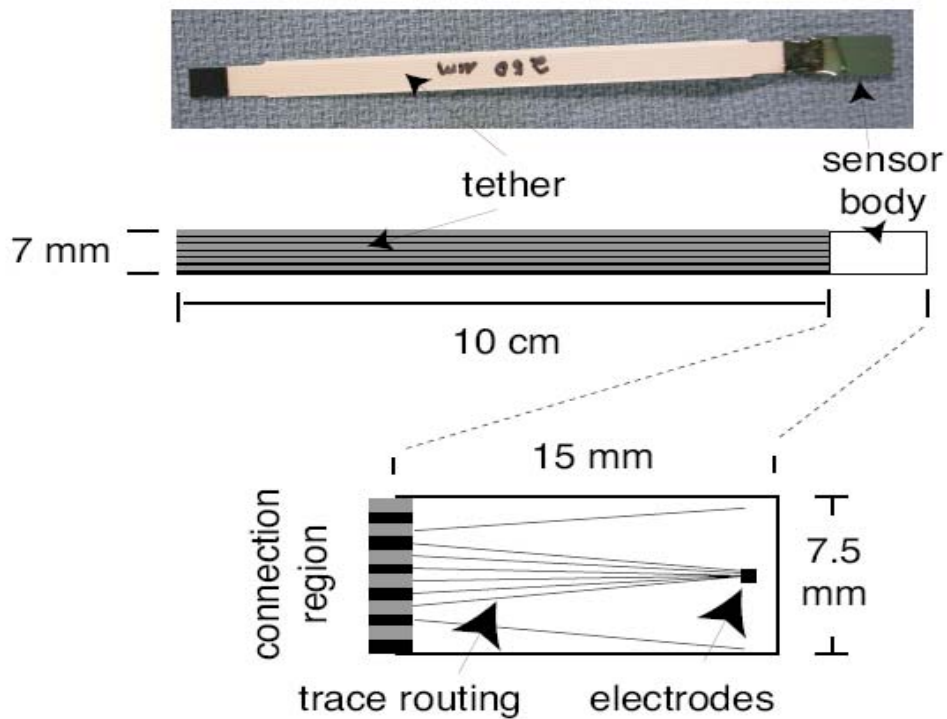


Figure 3.1 Assembly of the electrode array.

A close up view of the sensor body is shown in Figure 3.2.

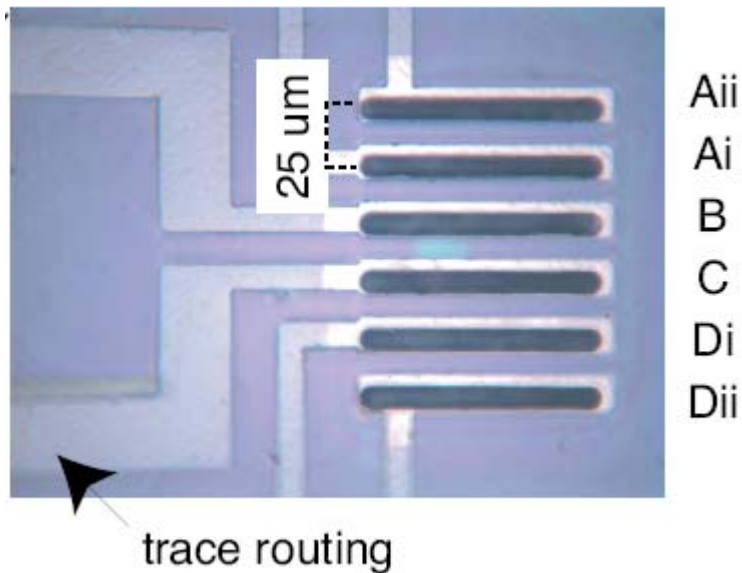


Figure 3.2 Close up view of platinum black electroplated arrays.

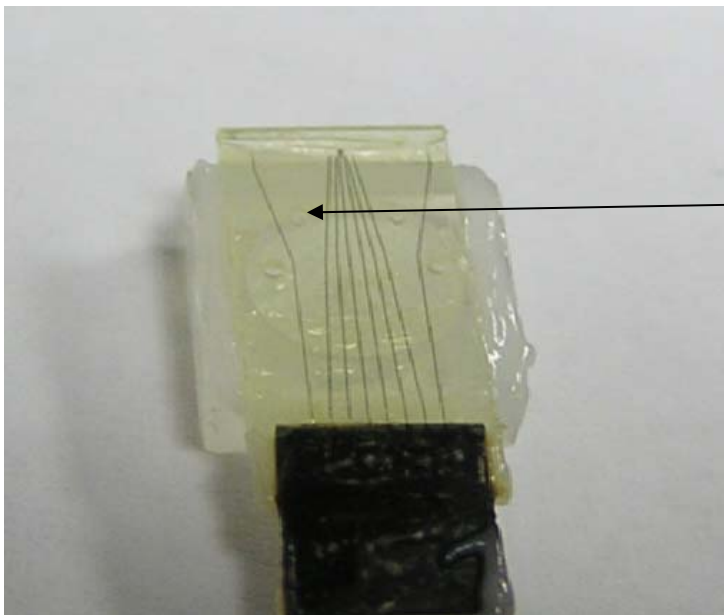
Microelectrode arrays fabricated on glass substrates have considerable advantages when compared to the assembly on silicon substrates. The electrodes fabricated on glass are capable of vacuum attachment in the heart tissue which reduces the tissue damage caused by the attachment of electrodes by suturing. The transparent glass substrate helps the user in accurate placement of the electrode array in the desired location when compared to the silicon electrode arrays. The electrical characteristics of the electrode arrays on both the silicon and the glass substrates remain the same.



Glass electrode body

Figure 3.3 Electrode array in glass substrates with vacuum attachment.

Four vacuum holes are drilled in the glass substrate as shown in Figure 3.4.



Vacuum Hole

Figure 3.4 Front side of the glass substrate showing four holes for vacuum attachment.



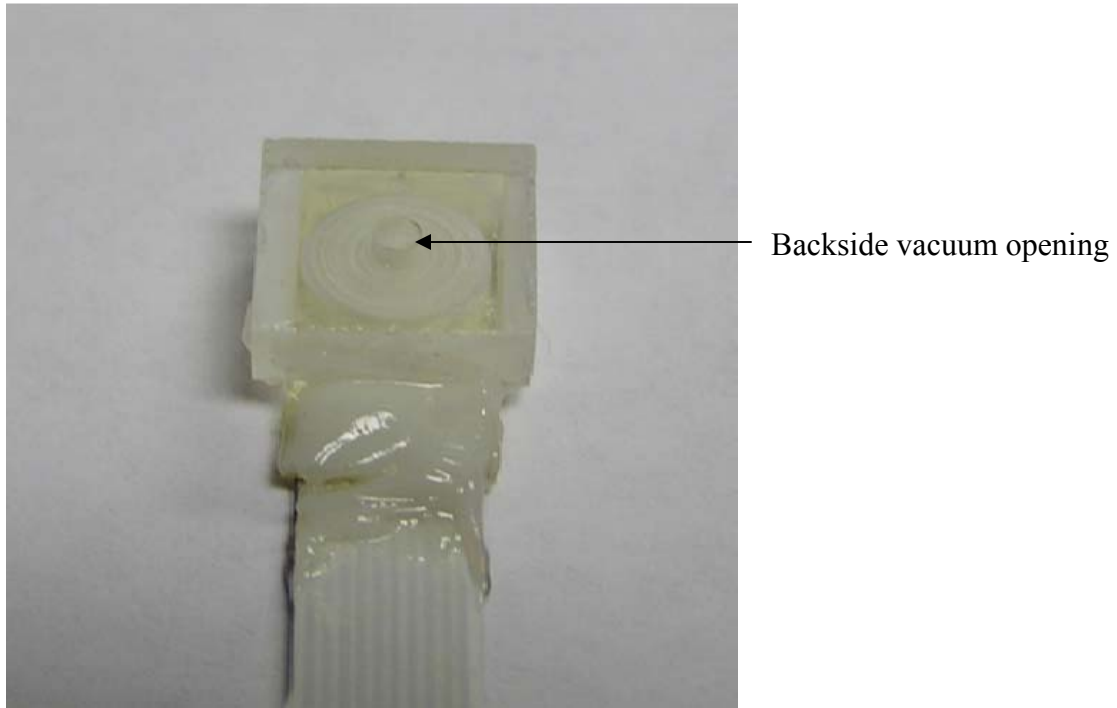


Figure 3.5 Backside of the glass substrate with vacuum attachment hole in glass piece.

### 3.2 Micro impedance Measurements

The micro impedance characterization of the fabricated electrodes is very important in determining whether they are suitable to use in the measurement of cardiac impedances with desirable signal to noise ratios. The impedance of the microelectrodes are tested on three different linear arrays of surface area of  $5\ \mu\text{m} \times 100\ \mu\text{m}$ ,  $5\ \mu\text{m} \times 250\ \mu\text{m}$ ,  $5\ \mu\text{m} \times 500\ \mu\text{m}$  with  $130\ \mu\text{m}$  spacings.

The electrodes are tested in a saline solution which is the commonly used electrolyte for electrophysiological studies. A unipolar stimulus with a sinusoidal voltage ( $V_{in}$ ) is supplied through a function generator at frequencies of 0.5, 5, 50 and 500 Hz to each electrode. The effective electrode impedance can be calculated from the equivalent

circuit shown in Figure 3.6. Any contribution to the effective impedance value from the solution to the reference is ignored due to the intrinsic low resistivity of the solution.

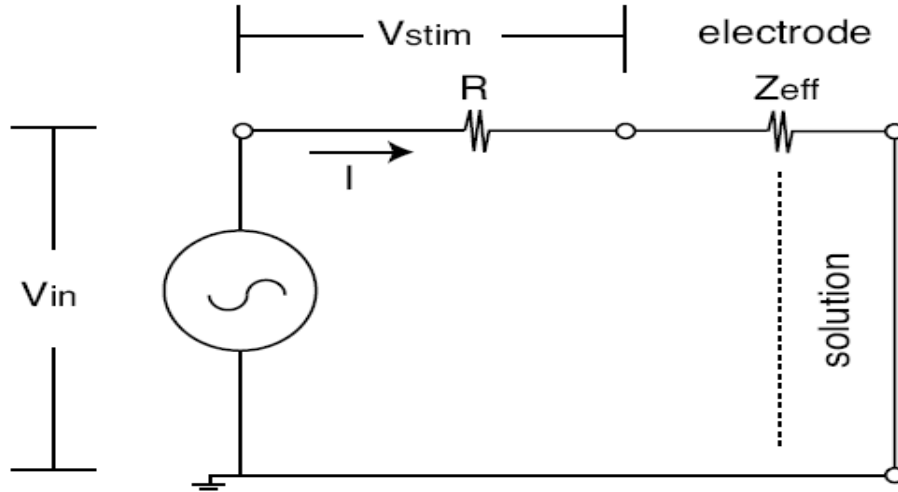


Figure 3.6 Equivalent circuit for electrode impedance measurement.

The effective impedance can be calculated by solving the equivalent circuit and is given

by 
$$Z_{eff} = R (V_{in}/V_{stim} - 1).$$

The plot of effective impedance  $Z_{eff}$  versus stimulation frequency is given in Figure 3.7.

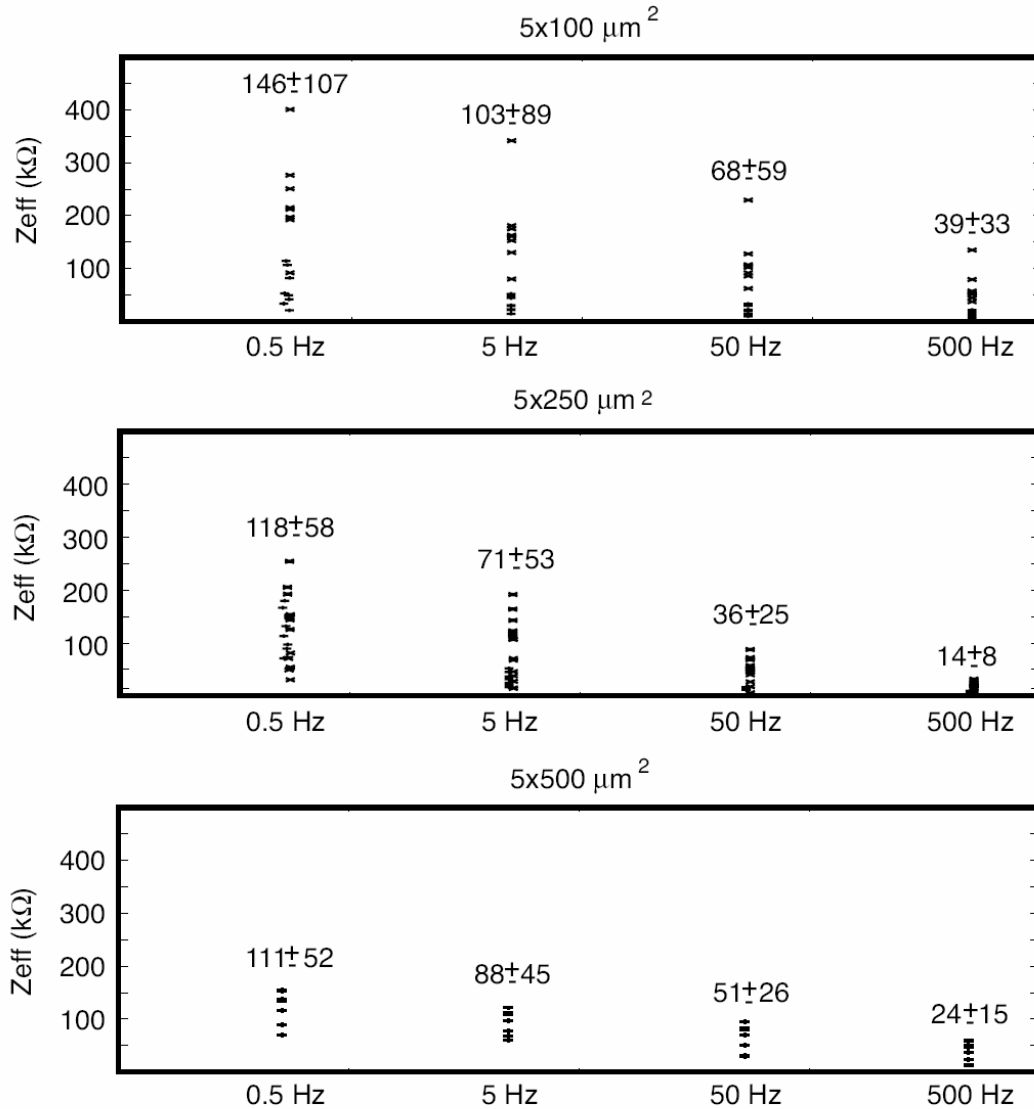


Figure 3.7 Impedance versus frequency plot, label values are mean and standard deviation.

With reference to Figure 3.7, the effective impedance value  $Z_{eff}$  plotted as a function of stimulation frequency shows there is a decrease in effective impedance as the frequency increases. The decrease in effective impedance is because as the frequency increases the capacitive reactance decreases.

The value of effective impedances achieved by this testing closely matches the effective impedances values of microelectrodes in the reports that were used for cardiac tissue preparations. Kim et al reported effective impedance of 5 Mohm at 10 Hz with 177 $\mu$ m iridium sensors, Chen et al reported effective impedance of 10 Mohm at 10 Hz with 1600 platinum sensors and Pollard et al reported effective impedance of 1.2 Mohm with 1963  $\mu$ m chloridized silver electrodes. The effective impedance for the electrodes fabricated in this work ranged from a maximum of 103 kohm at 50 Hz for 5x100  $\mu$ m electrodes to a minimum of 36 kohm at 50 Hz for 5  $\mu$ m x 250  $\mu$ m electrodes. The results from the impedance testing show that the 5  $\mu$ m x 100  $\mu$ m electrodes will be sufficient to make cardiac measurements and it may be possible in future work to further reduce the surface area of the electrodes and still achieve acceptable effective impedance values at the available electrode density. The main reason for the achieved impedance values are due to platinum black electroplating of the electrodes, which provides a highly porous surface which increases, the effective surface area, which in turn reduces the value of effective impedance.

### **3.3 Potential Difference Recordings**

The second test of the ability of the electrodes for stimulation and recording within cardiac space constants is to characterize the signal noise (SN) for  $\delta\Phi$  (surface potential) recorded in the solution. The importance of characterizing SN is that it will establish the accuracy of the measurement of  $\delta\Phi$  by the electrodes, since very accurate measurement of the surface potential amplitude will be critical in the measurement of cardiac micro impedances. Signal Noise (SN) calculated in these experiments document

the maximum possible deviation of the surface potential amplitudes from the actual values. The signal noise characterization was done in electrodes with three different surface areas which had the lowest overall effective impedance values. To record the  $\delta\Phi$ , voltages at the electrodes B and C were routed through a buffer amplification stage that incorporated a high pass filter of cutoff frequency 0.05 Hz to eliminate DC offset and maintain high input impedance for the second stage amplification with a low noise instrumentation amplifier. The stimulation current was supplied through either electrode A1 or A2 with D1 or D2 being the reference. Data from stimulating electrode combinations were collected at frequencies 0.5 Hz and 500 Hz.

### 3.4 Signal Noise Measurements

To measure the signal noise SN the value of each digitized  $\delta\Phi$  was compared with the associated  $V_{in}$  waveform. Figure 3.8 shows the steps used for that comparison, with an example obtained during Ai-Di stimulation at 0.5 Hz using  $5\ \mu\text{m} \times 100\ \mu\text{m}$  electrodes.

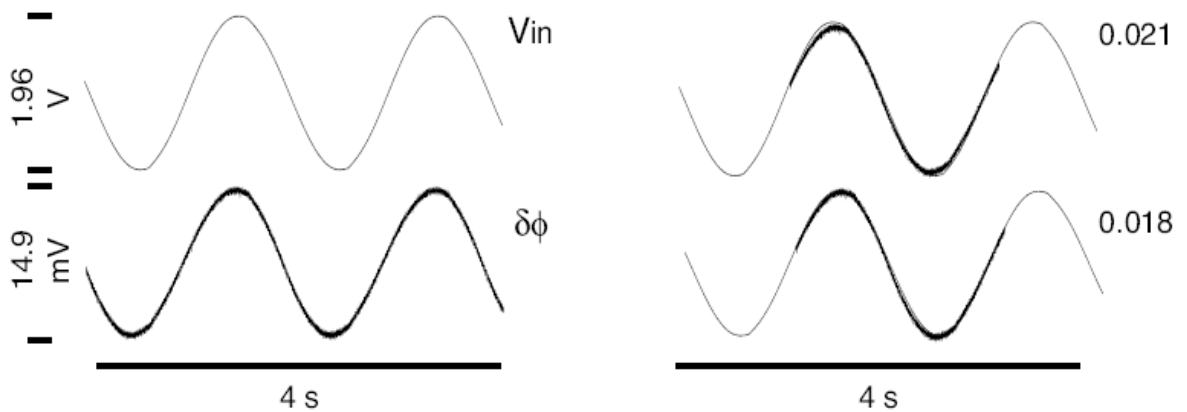


Figure 3.8 Signal Noise Measurements for Surface Potentials.

The left portion shows the  $V_{in}$  waveform above the  $\delta\Phi$  record, which had peak to peak amplitudes of 1.96 V and 14.9 mV, respectively. By comparison with  $\delta\Phi$ ,  $V_{in}$  is observed to be relatively noise free. To compare  $V_{in}$  and  $\delta\Phi$ , they are scaled to the range from 0 to 1 as shown in figure 3.8 and the root mean square difference is calculated between the scaled signals. The value is shown in the top right part of figure 8 which measured 0.021. The presence of noise in the  $\delta\Phi$  record influenced the comparison, as the scaled  $V_{in}$  samples deviated from the scaled  $\delta\Phi$  values near the peak of these records. Therefore  $V_{in}$  was rescaled to a range from 0.005 and 0.995 and a new root mean square difference was calculated, which is less than that from the original comparison. The procedure was repeated using 0.005 increments for the lower bound of the range of  $V_{in}$  and 0.005 decrements for the upper bound of the range of  $V_{in}$  until the root mean square difference is minimized. The bottom right portion of figure 8 shows the scaled  $\delta\Phi$  and  $V_{in}$  samples at which this minima was found for this example. The root mean square difference was 0.018 when scaled  $V_{in}$  ranged between 0.020 and 0.98. The  $\delta\Phi$  amplitude was therefore taken as the peak to peak for the original  $\delta\Phi$  record scaled by the  $V_{in}$  range i.e.  $(0.96) (14.9\text{mV}) = 14.3\text{mV}$ . Therefore signal noise (SN) is  $(0.018) (14.3\text{mV}) = 0.26\text{mV}$ .

### 3.5 Noise Levels

Using the procedure describe in the above section, Signal Noise was measured for the three different electrode sizes. Figure 3.9 shows the signal noise plotted against

frequency for  $\delta\Phi$  collected using  $5\ \mu\text{m} \times 100\ \mu\text{m}$ ,  $5\ \mu\text{m} \times 250\ \mu\text{m}$  and  $5\ \mu\text{m} \times 500\ \mu\text{m}$  electrodes. The average with the standard deviation for each electrode size is noted for each frequency tested. The low noise demonstrated in the above section was typical of SN because all the observed Signal Noise was below 1mV. The low average values of SN measured in these studies demonstrate the accuracy with which the surface potential amplitudes can be identified using the microfabricated electrode arrays.

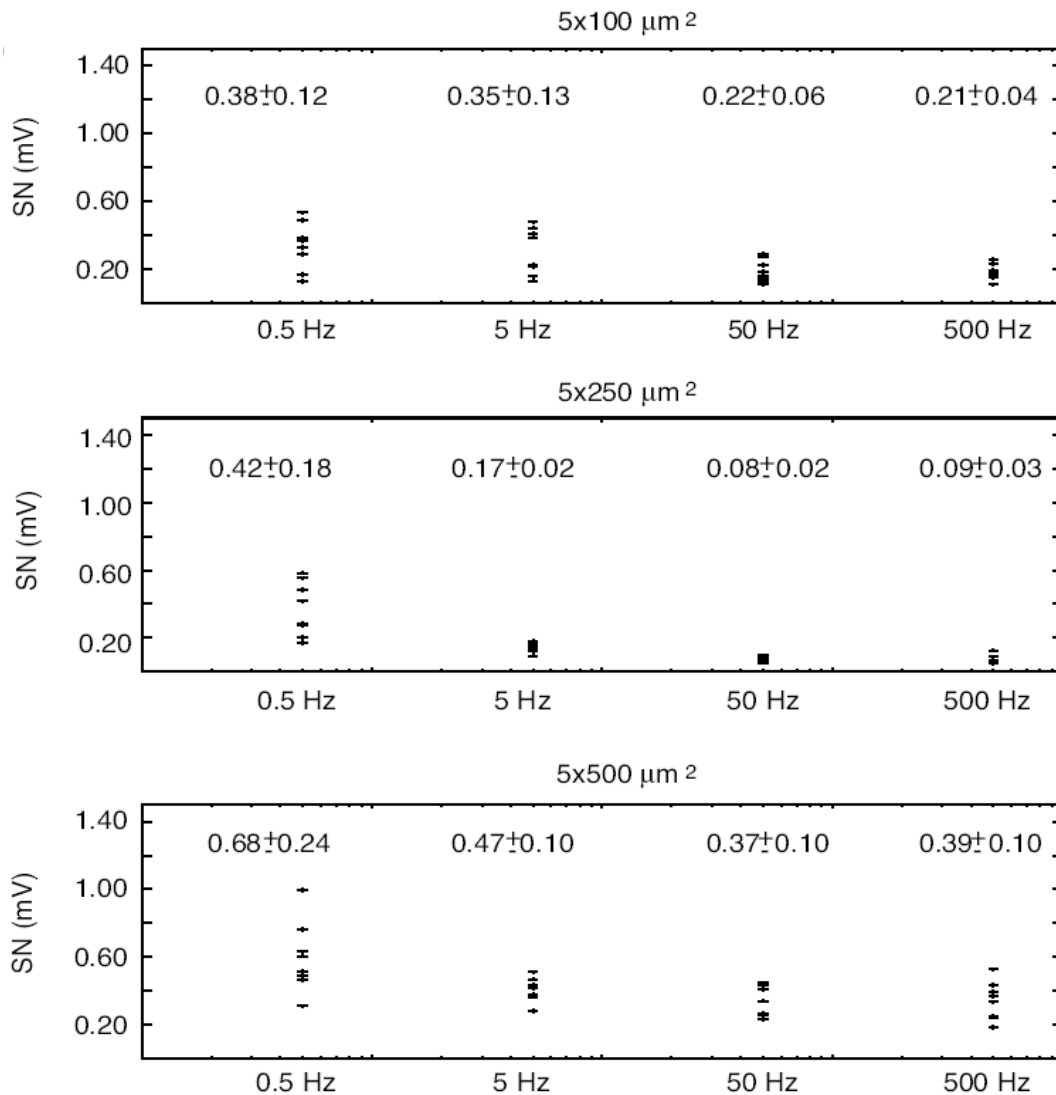


Figure 3.9 Signal Noise versus Frequency Plot for Surface Potentials.

## **CHAPTER 4**

### **CONCLUSIONS AND FUTURE WORK**

This research project demonstrates a method for building microelectrode arrays by micromachining techniques. This method is suitable for making cardiac electrophysiological measurements, as determined by measurements of effective impedance and signal noise. The low overall effective impedances of the electrodes facilitate high quality recordings of the surface potential with high quality signal noise characteristics during action potential propagation on a microscopic scale. The low noise levels achieved with these electrodes is very significant because during tissue experiments noise signals affect the measurements considerably. The effective impedance and noise levels suggest that it would be possible to make cardiac electrophysiological measurements with electrodes with even smaller dimensions, which could eventually lead to three dimensional electrodes. These electrode arrays have the potential to achieve multi-site stimulation in cardiac tissues.

The assembly of the microelectrodes on glass substrates with vacuum attachment helps in accurate placement of the electrodes with minimal tissue damage. The vacuum holes in the glass electrodes leave a fiducial mark in the cardiac tissue which will be helpful in performing repeated testing in the desired location in the tissue. There is a



potential to improve the assembly of the microelectrodes by fabricating the electrodes on flexible thin polyimide film which will reduce the problems associated with positioning of the electrodes during cardiac electrophysiology experiments.

The electrode fabrication process can be optimized to improve the durability of the electrodes. The platinum black which is electroplated on the gold layer tends to disintegrate because of repeated use in the saline solution. Identifying the reason for this occurrence and the improvement in the plating process will make the arrays more durable by preserving the required electrical characteristics of the electrode. The electrode arrays can be fabricated in three dimensional structures to further increase the electrode surface area.

## REFERENCES

- [1] Heikki V. Huikkuri, Agustin Castellanos and Robert J. Myerburg, "Sudden Death due to Cardiac Arrhythmias," *New England Journal of Medicine*, Vol. 345, No.20, 2001.
- [2] Robert Plonsey and Roger C. Barr, "Bioelectricity: a Quantitative Approach"
- [3] Robert Plonsey and David G. Fleming, "Bioelectric Phenomena"
- [4] J.James Wiley, Raymond E. Ideker, William M. Smith and Andrew E. Pollard, "Measuring surface potential components necessary for transmembrane current density computation using microfabricated arrays", *American Journal of Physiology*, Vol 289:2468-2477, 2005.
- [5] Andrew E. Pollard and Roger c. Barr, "Cardiac Microimpedance Measurement in two dimensional models using multisite stimulation", *American Journal of Physiology*, Vol 290:1976-1987, 2005.
- [6] Seung-joon Paik, Yonghwa Park and Dong-il Cho, "Roughened polysilicon for low impedance microelectrodes in neural Probes", *Journal of Micromechanics and Microengineering*, Vol 13: 373-379, 2003.
- [7] Andy Hung, David Zhou, Robert Greenberg and Jack W. Judy, "Micromachined electrodes for Retinal Prosthesis", *Conference on microtechnologies in medicine and biology*, May2-4 2002.

- [8] Chen, X, Lal, A, Riccio, ML, and Gilmour, RF, “ultrasonically actuated silicon microprobes for cardiac signal recording”, IEEE Transactions on. Biomedical Engineering. Vol 53:1665-1671, 2006.
- [9] Kim, C-S, Ufer, S, Seagle, CM, Engle, CL, Nagle, HT, Johnson, TA, and Cascio, WE, “Use of micromachined probes for the recording of cardiac electrograms in isolated heart tissues”, Biosens. Bioelectron. 19:1109-1116, 2004.
- [10] L.S. Robblee, J. McHardy, W.F. Agnew, and L.A. Bullara, "Electrical stimulation with Pt electrodes. VII. Dissolution of Pt electrodes during electrical stimulation of the cat cerebral cortex," *Journal of Neuroscience Methods*, vol. 9, no. 4, December 1983.
- [11] John J. Whalen III, Jeffrey Young, James D. Weiland, and Peter C. Searson, “Electrochemical Characterization of Charge Injection at Electrodeposited Platinum Electrodes in Phosphate Buffered Saline”, *Journal of the Electrochemical Society*, 153, 12 C834-C839, 2006.
- [12] M.A. Petit and V. Plichon, "Anodic electrodeposition of iridium oxide films," *Journal of Electroanalytical Chemistry*, vol. 444, pp. 247-252, October 1997.
- [13] <http://www.rush.edu/rumc/page-1098987312456.html>
- [14] Richard C Jaeger, *Introduction to Microelectronic Fabrication*, Addison-Wesley, 1998.